« JOMP 10915 layout: Small Condensed v.1.2 file: jomp9524.tex (ELE) class: spr-small-v1.1 v.2011/08/17 Prn:2011/08/18; 11:21 p. 1/19»
« doctopic: OriginalPaper numbering style: ContentOnly reference style: mathphys»

J Sci Comput
DOI 10.1007/s10915-011-9524-0

Iterative Design of Concentration Factors for Jump Detection

Adityavikram Viswanathan · Anne Gelb · Douglas Cochran

Received: 2 December 2010 / Accepted: 27 July 2011

Abstract The concentration method of edge detection was developed to compute the locations and values of jump discontinuities in a piecewise-analytic function from its first few Fourier series coefficients. The accuracy and characteristic features of the resulting jump approximation depend on Fourier space "filter" factors known as concentration factors. In this paper, we provide a flexible, iterative framework for the design of these factors. Previously devised concentration factors are shown to be the solutions of specific problem formulations within this new framework. We also provide sample formulations of the procedure applicable to the design of concentration factors for data with missing spectral bands. Several illustrative examples are used to display the capabilities of the method.

Keywords Jump detection · Concentration edge detection · Convex optimization

1 Introduction

Detection and characterization of abrupt changes in signals are important in many signal processing applications. A sudden change in the amplitude of a one-dimensional signal often indicates a significant transition in the state of the signal source, such as catastrophic failure of a component in a mechanical or electrical system. Accurate estimation of the time of the

This work was supported in part by National Science Foundation grants CNS 0324957, DMS 0510813 and FRG 0652833.

A. Viswanathan (✉) · D. Cochran
School of Electrical, Computer & Energy Engineering, Arizona State University, Tempe, AZ 85287-5706, USA
e-mail: aditya.v@asu.edu

D. Cochran
e-mail: cochran@asu.edu

A. Gelb
School of Mathematical and Statistical Sciences, Arizona State University, Tempe, AZ 85287-1804, USA
e-mail: ag@math.la.asu.edu

Journal ID: 10915, Article ID: 9524, Date: 2011-08-19, Proof No: 1

« JOMP 10915 layout: Small Condensed v.1.2 file: jomp9524.tex (ELE) class: spr-small-v1.1 v.2011/08/17 Prn:2011/08/18; 11:21 p. 2/19»
« doctopic: OriginalPaper numbering style: ContentOnly reference style: mathphys»

leading edge of an emitted radar pulse at multiple distributed receivers provides a means for passive localization of the emitter. In image processing and other multi-dimensional applications, detection of sharp transitions is valuable for segmentation and descriptors of edges and other abrupt phenomena in data are often used as features in pattern recognition. In the solution of PDEs using spectral methods, identification of jump discontinuities and associated processing can greatly improve the accuracy of the solutions.

In some of these cases, we may be required to identify jumps in the data given measurements in the Fourier domain. This is the case in applications such as magnetic resonance imaging (MRI) and synthetic aperture radar (SAR). The underlying physics of these problems models the signal acquisition process as the collection of samples of the Fourier transform of the specimen being imaged. The detection of jumps from such data is a challenging problem, since Fourier data constitutes a global representation, from which we seek accurate representations of a local phenomenon.

The concentration method of edge detection, [1], was devised with exactly this in mind. It computes an approximation to what is known as the *jump function* (defined in Sect. 2) from the first $2N+1$ Fourier series coefficients of the function using a partial Fourier sum and Fourier space "filter" factors known as *concentration factors*. The characteristic properties of the resulting approximation, including the behaviors in the neighborhood of jumps and smooth regions away from jumps, are determined by these factors. In this paper, we present an iterative framework for the design of these factors. Admissible concentration factors are shown to be generated by solving an iterative, and typically convex program. Some of the traditional concentration factors, originally derived in [1, 2], are shown to be the solutions of particular problem formulations within our new framework. In addition, this framework admits the design of factors satisfying specific constraints with regard to the resulting jump approximation. We also present the application of this framework to the design of concentration factors with missing or banded spectral data. Unavailability of data in some frequency bands is common in practice due to several causes, including limitations in sensor capability, the presence of strong incidental or intentional narrowband interference, and communication link restrictions or dropouts.

The rest of the paper is organized as follows. Section 2 summarizes the concentration edge detection method, including the notion of a jump function, concentration factors and their admissibility conditions. A few prototypical families of concentration factors are tabulated and their performance on test functions illustrated. The notion of *low* and *high order* edge detectors is also briefly explained. Section 3 starts by providing a summary of previous and related work on the topic, before introducing our new framework of concentration factor design. This section contains several sample problem formulations which illustrate the flexibility of the framework, while also serving to associate some of the traditional concentration factors with specific iterative formulations. Section 4 examines the application of the framework to missing or banded spectral data. We give some concluding comments and avenues for future investigation in Sect. 5.

2 The Concentration Edge Detection Method

Let f be a 2π-periodic piecewise-smooth function[1] defined in $[-\pi, \pi)$. We will assume that we are given the Fourier series coefficients

[1] We restrict our attention to real-valued functions, since practical applications typically demand the identification and characterization of real-valued jumps.

Journal ID: 10915, Article ID: 9524, Date: 2011-08-19, Proof No: 1, UNCORRECTED PROOF

$$\hat{f}(k) = \frac{1}{2\pi}\int_{-\pi}^{\pi} f(x)e^{-ikx}\,dx, \quad k = -N, \ldots, N. \tag{1}$$

Definition 1 (Jump Function) Let the right and left-hand limits of the function, $f(x^+)$ and $f(x^-)$, be defined at every point x in the domain. The jump function associated with f and denoted by $[f]$ is defined as the difference between the right and left hand limits of the function at every point x; i.e.,

$$[f](x) := f(x^+) - f(x^-). \tag{2}$$

Note that the jump function is non-zero only at a jump discontinuity, where it takes the value of the jump.

Given the first $2N+1$ Fourier coefficients of a piecewise-smooth function, the concentration edge detection method, [1, 2], computes an approximation to the jump function using a partial sum of the form

$$S_N^\sigma[f](x) = i\sum_{|k|\le N} \hat{f}(k)\mathrm{sgn}(k)\sigma\left(\frac{|k|}{N}\right)e^{ikx}. \tag{3}$$

The convergence properties of the jump approximation depend on the choice of factors $\sigma(\eta) = \sigma(\frac{|k|}{N})$, which are known as *concentration factors*. These factors satisfy certain admissibility conditions which are enumerated below. The interested reader is referred to [2] for more details.

1. $\sum_{k=1}^{N}\sigma(\frac{k}{N})\sin(kx)$ be odd
2. $\frac{\sigma(\eta)}{\eta} \in C^2(0,1)$
3. $\int_\epsilon^1 \frac{\sigma(\eta)}{\eta} \to -\pi, \epsilon = \epsilon(N) > 0$ being small

It is illustrative to note that the equivalent physical-space representation of the concentration sum in (3) is the convolution of f with a *concentration kernel* C_N^σ defined as

$$C_N^\sigma(x) := i\sum_{|k|\le N} \mathrm{sgn}(k)\sigma\left(\frac{|k|}{N}\right)e^{ikx}. \tag{4}$$

Thus (3) is equivalent to

$$S_N^\sigma[f](x) = (f * C_N^\sigma)(x). \tag{5}$$

The admissibility conditions simply state that this kernel is required to be odd and suitably normalized in order to approximate the jump function. A certain amount of smoothness is also required as enumerated by condition 2. If these conditions are satisfied, $S_N^\sigma[f]$ "concentrates" at the singular support of f and the jump approximation obeys the concentration property, [5, Theorem 2.3],

$$S_N^\sigma[f](x) = [f](x) + \begin{cases} \mathcal{O}\left(\frac{\log N}{N}\right) & d(x) \lesssim \frac{\log N}{N} \\ \mathcal{O}\left(\frac{\log N}{(Nd(x))^s}\right) & d(x) \gg \frac{1}{N}. \end{cases} \tag{6}$$

Here, $d(x)$ denotes the distance between a point in the domain and the nearest discontinuity, while $s > 0$ depends on the concentration factor chosen. Use of a *higher-order*[2] edge detec-

[2]The notion of low and high order edge detectors and their characteristic features will be discussed below.

Table 1 Examples of concentration factors

Factor	Expression	Remarks
Trigonometric	$\sigma_G(\eta) = \frac{\pi \sin(\pi\eta)}{\mathrm{Si}(\pi)}$	$\mathrm{Si}(\pi) = \int_0^\pi \frac{\sin(x)}{x}\,dx$
Polynomial	$\sigma_P^p(\eta) = p\pi\eta^p$	p is the order of the factor
Exponential	$\sigma_E(\eta) = C\eta e^{(\frac{1}{\alpha\eta(\eta-1)})}$	α is the order C is a normalizing constant $C = \frac{\pi}{\int_{\frac{1}{N}}^{1-\frac{1}{N}} \exp(\frac{1}{\alpha\tau(\tau-1)})d\tau}$

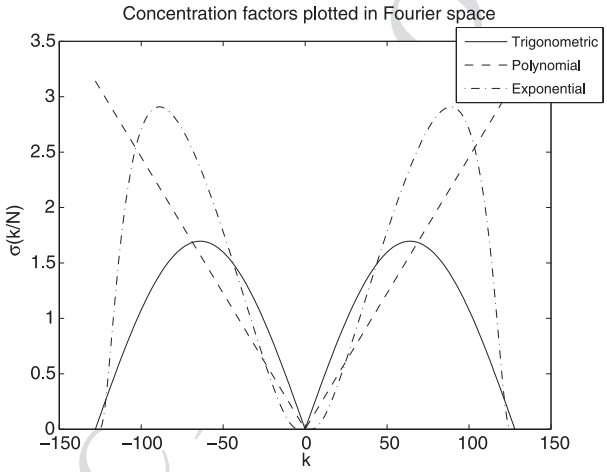

Fig. 1 Concentration factors plotted in Fourier space, $N = 128$

tor results in a larger value of s as compared to using a *lower-order* edge detector. Table 1 lists a selection of concentration factors introduced in [1, 2], while Fig. 1 plots these factors in the Fourier domain.

Each concentration factor generates a unique oscillatory response in the immediate vicinity and away from jumps. We will refer to this as the *jump response* associated with a concentration factor.

Let $\sigma(\eta)$ be an admissible concentration factor. Let $r(x)$ denote the unit ramp function, with a corresponding jump function $[r](x)$.

$$r(x) = \begin{cases} \frac{-x-\pi}{2\pi} & x < 0 \\ \frac{\pi-x}{2\pi} & x > 0 \end{cases}, \qquad [r](x) = \begin{cases} 1 & x = 0 \\ 0 & \text{else.} \end{cases}$$

Definition 2 (Jump Response) The jump response, denoted by $W_0^{\sigma,N}(x)$, is defined as the jump function approximation of the unit ramp as generated by the concentration sum (3). i.e.,

$$W_0^{\sigma,N}(x) := S_N^\sigma[r](x) = i \sum_{|k|\le N} \hat{r}(k)\mathrm{sgn}(k)\sigma\left(\frac{|k|}{N}\right)e^{ikx}$$

$$= \frac{1}{2\pi} \sum_{0<|k|\le N} \frac{\sigma(\frac{|k|}{N})}{|k|} e^{ikx}. \tag{7}$$

« JOMP 10915 layout: Small Condensed v.1.2 file: jomp9524.tex (ELE) class: spr-small-v1.1 v.2011/08/17 Prn:2011/08/18; 11:21 p. 5/19»
« doctopic: OriginalPaper numbering style: ContentOnly reference style: mathphys»

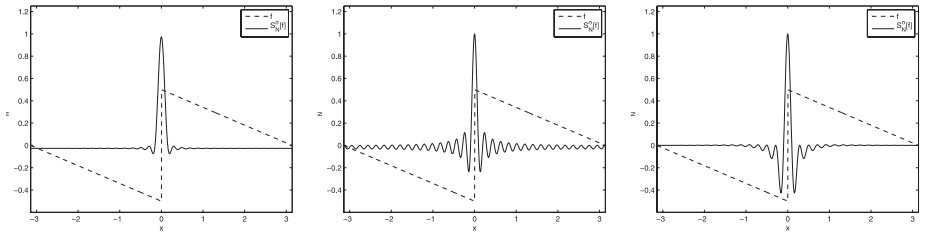

(a) Trigonometric (b) Polynomial (c) Exponential

Fig. 2 Characteristic responses of different concentration factors to a sawtooth function ($N = 32$)

The final equation is obtained by substituting the Fourier coefficients of the ramp function,

$$\hat{r}(k) = \begin{cases} \frac{1}{2\pi i k} & k \neq 0 \\ 0 & k = 0. \end{cases}$$

The jump responses of each of the concentration factors listed in Table 1 are plotted in Fig. 2. These plots serve to illustrate the "concentration" of the jump approximation at the jump location. Note also the non-uniform convergence to the true jump function, as stated in (6). The different orders of convergence away from the jump for each of the concentration factors, parameterized by s in (6), is also seen from the plots. For example, the polynomial concentration factor shows slowly decaying oscillations for $|x| > 0$, while the exponential factor shows a vanishing response away from the jump.

As evidence of the use of this method on more general functions, consider the jump approximations of the two test functions in (8) and (10), plotted in Fig. 3(a) and (b) respectively. The true jump functions are provided for reference in (9) and (11) respectively.

$$f_1(x) = \begin{cases} \frac{3}{2} & -\frac{3\pi}{4} \leq x < -\frac{\pi}{2} \\ \frac{7}{4} - \frac{x}{2} + \sin(x - \frac{1}{4}) & -\frac{\pi}{4} \leq x < \frac{\pi}{8} \\ \frac{11}{4}x - 5 & \frac{3\pi}{8} \leq x < \frac{3\pi}{4} \\ 0 & \text{else.} \end{cases} \tag{8}$$

$$[f_1](x) = \begin{cases} \frac{3}{2} & x = -\frac{3\pi}{4} \\ -\frac{3}{2} & x = -\frac{\pi}{2} \\ \frac{14+\pi}{8} - \sin\left(\frac{\pi+1}{4}\right) \approx 1.28 & x = -\frac{\pi}{4} \\ \sin\left(\frac{2-\pi}{8}\right) - \frac{28-\pi}{16} \approx -1.70 & x = \frac{\pi}{8} \\ \frac{33\pi}{32} - 5 \approx -1.76 & x = \frac{3\pi}{8} \\ 5 - \frac{33\pi}{16} \approx -1.48 & x = \frac{3\pi}{4} \\ 0 & \text{elsewhere.} \end{cases} \tag{9}$$

$$f_2(x) = \begin{cases} \sin(6x) & -\frac{5\pi}{6} \leq x < 0 \\ \frac{1}{\pi}e^{-2x}(\pi - x) & x \geq 0. \end{cases} \tag{10}$$

Journal ID: 10915, Article ID: 9524, Date: 2011-08-19, Proof No: 1, UNCORRECTED PROOF

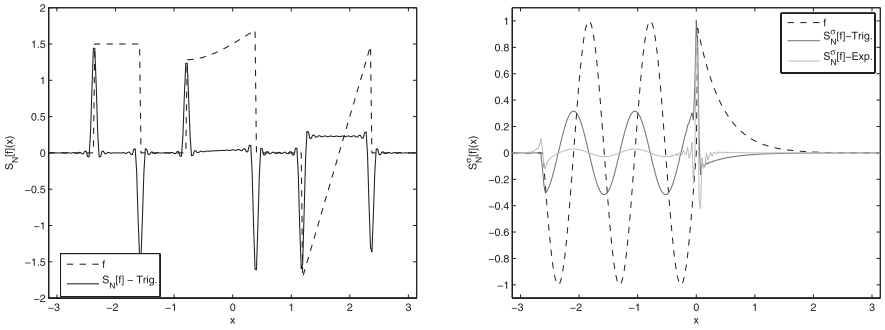

(a) Jump approximation of $f_1(x), N = 64$ (b) Jump approximation of $f_2(x), N = 100$

Fig. 3 Jump approximations of two test functions

$$[f_2](x) = \begin{cases} 1 & x = 0 \\ 0 & \text{else.} \end{cases} \tag{11}$$

The jump function approximation of $f_1(x)$ was generated using the trigonometric factor while the trigonometric and exponential jump function approximations of $f_2(x)$ are plotted. Note that the trigonometric jump function approximation of $f_2(x)$ has a significant non-zero value in the smooth interval $(-\pi, 0)$. This is an example of a *low-order* edge detector acting on a function with large variation. In comparison, the response using the exponential (*high-order*) factor contains minimal spurious responses in smooth regions[3] at the expense of some additional oscillatory behavior in the immediate vicinity of a discontinuity. Moreover, since the function has significant variation, a larger number of Fourier modes ($N = 100$) are necessary to recover a well resolved jump function approximation.

3 Concentration Factor Design

We start this section by providing a brief summary of previous and related work on this topic. Since the initial development of the concentration edge detection method in [1, 2], several works have addressed the improvement in the resolution of jump approximations. A survey of related literature reveals two broad approaches—enhancements and reformulations of the concentration method itself, and design of new families of concentration factors. Enhancements to the concentration method include nonlinear post-processing procedures such as enhancement of scales, [2], which separates regions (or scales) of jumps from regions of smoothness by raising the jump approximation to a power. As indicated previously and plotted in Figs. 2 and 3, the different concentration factors are characterized by their behavior in the vicinity of a jump and in smooth regions. Use of a multitude of jump responses in conjunction with the *minmod* operator is treated in [3]. This results in fewer oscillations near a jump as well as removal of spurious responses in smooth regions. Iterative formulations of the concentration method with connections to the recently developed theory of compressive sensing, [8, 9] were introduced in [7]. Here, pre-existing families of concentration factors

[3]The small non-zero oscillatory response in the vicinity of $x = -\frac{5\pi}{6}$ is due to a discontinuity in the derivative of $f_2(x)$.

Journal ID: 10915, Article ID: 9524, Date: 2011-08-19, Proof No: 1, UNCORRECTED PROOF

« JOMP 10915 layout: Small Condensed v.1.2 file: jomp9524.tex (ELE) class: spr-small-v1.1 v.2011/08/17 Prn:2011/08/18; 11:21 p. 7/19»
« doctopic: OriginalPaper numbering style: ContentOnly reference style: mathphys»

were utilized in sparsity-enforcing formulations of the concentration method to yield accurate approximations to the jump function. This method also allows for the detection of edges from highly incomplete Fourier measurements.

Select literature on the design of new concentration factors can also be found. For example, a family of concentration factors known as matching waveform concentration factors was developed in [4]. These look for correlations in the concentration jump approximation with the jump response of the concentration factor, and results in approximations with reduced oscillatory behavior. The design of concentration factors for noisy data is treated in [5]. The approach in [5] is based on separating the Fourier data into scales of "smoothness", noise and the jump discontinuity. An alternate approach to reducing the effects of noise in concentration edge detection and reconstruction is explained in [6]. We note that each of these works describes the design of a single family of concentration factor. Our present work, in comparison, is more general in formulation and allows for the realization of multiple families of concentration factors.

We start our discussion of concentration factor design by obtaining an expression relating the jump function to the concentration jump response. Consider a periodic function on $[-\pi,\pi)$ with a single jump at $x=\zeta$. We remark that this discussion may be easily generalized to the case of multiple jumps, as long as any two jumps are separated by a distance greater than $\mathcal{O}(\frac{\log N}{N})$. We start by expressing the Fourier coefficients in terms of the jump locations and values. For $k\neq 0$, we have

$$\hat{f}(k)=\frac{1}{2\pi}\int_{-\pi}^{\zeta^-} f(x)e^{-ikx}dx+\frac{1}{2\pi}\int_{\zeta^+}^{\pi} f(x)e^{-ikx}dx. \tag{12}$$

On integrating by parts, we obtain

$$\hat{f}(k)=\left(f(\zeta^+)-f(\zeta^-)\right)\frac{e^{-ik\zeta}}{2\pi ik}+\frac{1}{ik}\cdot\left(\frac{1}{2\pi}\int_{-\pi}^{\zeta^-} f'(x)e^{-ikx}+\frac{1}{2\pi}\int_{\zeta^+}^{\pi} f'(x)e^{-ikx}\right), \tag{13}$$

where we have used the periodicity of f. From (2), we obtain

$$\hat{f}(k)=[f](\zeta)\frac{e^{-ik\zeta}}{2\pi ik}+\frac{1}{ik}\cdot\left(\frac{1}{2\pi}\int_{-\pi}^{\zeta^-} f'(x)e^{-ikx}+\frac{1}{2\pi}\int_{\zeta^+}^{\pi} f'(x)e^{-ikx}\right).$$

Note that the term within parenthesis is the same as (12) for f'. Therefore, by repeated application of integration by parts, we obtain

$$\hat{f}(k)=\frac{1}{2\pi}\left(\frac{[f](\zeta)}{ik}+\frac{[f'](\zeta)}{(ik)^2}+\frac{[f''](\zeta)}{(ik)^3}+\cdots\right)e^{-ik\zeta},\quad k\neq 0. \tag{14}$$

Let us now substitute this in the expression for the concentration sum in (3).

$$\begin{aligned}S_N^{\sigma}[f](x)&=\sum_{0<|k|\leq N}\hat{f}(k)i\sigma\left(\frac{|k|}{N}\right)\operatorname{sgn}(k)e^{ikx}\\&=\sum_{0<|k|\leq N}\left[\frac{1}{2\pi}\left(\frac{[f](\zeta)}{ik}+\frac{[f'](\zeta)}{(ik)^2}+\cdots\right)e^{-ik\zeta}\right]i\sigma\left(\frac{|k|}{N}\right)\operatorname{sgn}(k)e^{ikx}\\&=\frac{[f](\zeta)}{2\pi}\sum_{0<|k|\leq N}\frac{\sigma\left(\frac{|k|}{N}\right)\operatorname{sgn}(k)}{k}e^{ik(x-\zeta)}\end{aligned}$$

Journal ID: 10915, Article ID: 9524, Date: 2011-08-19, Proof No: 1, UNCORRECTED PROOF

$$+\frac{[f'](\zeta)}{2\pi}\sum_{0<|k|\le N}\frac{\sigma\left(\frac{|k|}{N}\right)\operatorname{sgn}(k)}{ik^2}e^{ik(x-\zeta)}$$

$$+\frac{[f''](\zeta)}{2\pi}\sum_{0<|k|\le N}\frac{\sigma\left(\frac{|k|}{N}\right)\operatorname{sgn}(k)}{i^2k^3}e^{ik(x-\zeta)}+\cdots. \tag{15}$$

Recall that the first term in the above equation is a shifted and scaled jump response, $W_0^{\sigma,N}$, (Definition 2). Similarly we may define

$$\frac{1}{2\pi}\sum_{0<|k|\le N}\frac{\sigma(\frac{|k|}{N})\operatorname{sgn}(k)}{ik^2}e^{ikx}:=W_1^{\sigma,N}(x), \tag{16}$$

and, in general,

$$\frac{1}{2\pi}\sum_{0<|k|\le N}\frac{\sigma\left(\frac{|k|}{N}\right)\operatorname{sgn}(k)}{i^qk^{q+1}}e^{ikx}:=W_q^{\sigma,N}(x). \tag{17}$$

Substituting in (15), we obtain

$$S_N^\sigma[f](x)=[f](\zeta)W_0^{\sigma,N}(x-\zeta)+[f'](\zeta)W_1^{\sigma,N}(x-\zeta)+[f''](\zeta)W_2^{\sigma,N}(x-\zeta)+\cdots. \tag{18}$$

We note that the jump "function" is in fact a quantity of zero measure, making the theoretical development and analysis of the method difficult. To overcome this, we follow [5] and similarly use a regularized equivalent of the jump function, which we denote by $[f]_\epsilon(x)$, and define as

$$[f]_\epsilon(x)=\begin{cases}[f](\zeta) & |x-\zeta|\le\epsilon,\ \epsilon>0,\ \epsilon\sim\mathcal{O}\left(\frac{2\pi}{2N+1}\right)\\ 0 & \text{else.}\end{cases} \tag{19}$$

Thus, (18) becomes

$$\begin{aligned}S_N^\sigma[f](x)\approx&[f]_\epsilon(\zeta)W_0^{\sigma,N}(x-\zeta)+[f']_\epsilon(\zeta)W_1^{\sigma,N}(x-\zeta)\\&+[f'']_\epsilon(\zeta)W_2^{\sigma,N}(x-\zeta)+\cdots\\\approx&\int_{-\pi}^{\pi}[f]_\epsilon(\zeta)W_0^{\sigma,N}(x-\zeta)d\zeta+\int_{-\pi}^{\pi}[f']_\epsilon(\zeta)W_1^{\sigma,N}(x-\zeta)\,d\zeta\\&+\int_{-\pi}^{\pi}[f'']_\epsilon(\zeta)W_2^{\sigma,N}(x-\zeta)\,d\zeta+\cdots\\=&([f]_\epsilon*W_0^{\sigma,N})(x)+([f']_\epsilon*W_1^{\sigma,N})(x)+([f'']_\epsilon*W_2^{\sigma,N})(x)+\cdots.\end{aligned} \tag{20}$$

From (16) and (17), we note that $W_i^{\sigma,N}(x)=(\tilde{B}_i*C_N^\sigma)(x)$, where $\tilde{B}_i(x)$ are normalized Bernoulli polynomials,[4] [13], and $C_N^\sigma(x)$ is the concentration kernel (4). Since $\tilde{B}_i(x)$ has a discontinuity in its ith derivative at $x=0$, each of these kernels denotes the response of the concentration sum to jumps in the i^{th} derivative of the function. Since we are interested in identifying jumps, we will call $W_0^{\sigma,N}$ as the jump response of the concentration method to a

[4]High-resolution reconstruction methods for discontinuous data based on subtracting out these Bernoulli polynomials have been pursued successfully in [13].

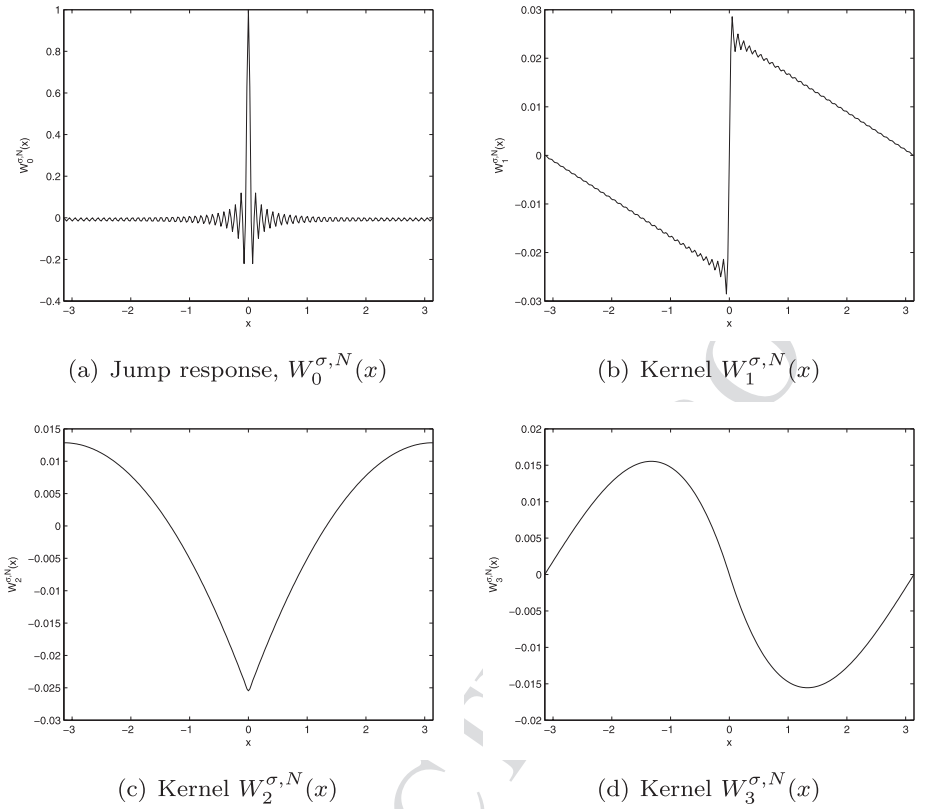

(a) Jump response, $W_0^{\sigma,N}(x)$ (b) Kernel $W_1^{\sigma,N}(x)$

(c) Kernel $W_2^{\sigma,N}(x)$ (d) Kernel $W_3^{\sigma,N}(x)$

Fig. 4 The jump response and first three higher order kernels associated with the polynomial concentration factor ($N = 64$)

unit jump or the "jump waveform". The jump response and the first three higher-order kernels associated with the polynomial concentration factor are plotted for illustrative purposes in Fig. 4. Note the alternating even-odd nature of the kernels and the reduced scale of the higher order kernel plots.

3.1 Framework for Concentration Factor Design

From the prior discussion, it is clear that the objective in concentration factor design is to emphasize $W_0^{\sigma,N}(x)$, while suppressing the impact of $W_i^{\sigma,N}(x)$, $i > 0$.[5] Further, for a faithful jump approximation, we require (from Definition 1) that $W_0^{\sigma,N}(x)$ have properties similar to the indicator function

$$\delta(x) = \begin{cases} 1 & x = 0 \\ 0 & \text{else.} \end{cases} \tag{21}$$

Consequently, the design framework consists of solving an iterative program which computes a concentration factor σ for (3) such that the above conditions are satisfied. A typical

[5]The necessity to suppress $W_i^{\sigma,N}(x), i > 0$ is evident in the jump function approximation of $f_2(x)$, plotted in Fig. 3(b).

« JOMP 10915 layout: Small Condensed v.1.2 file: jomp9524.tex (ELE) class: spr-small-v1.1 v.2011/08/17 Prn:2011/08/18; 11:21 p. 10/19»
« doctopic: OriginalPaper numbering style: ContentOnly reference style: mathphys»

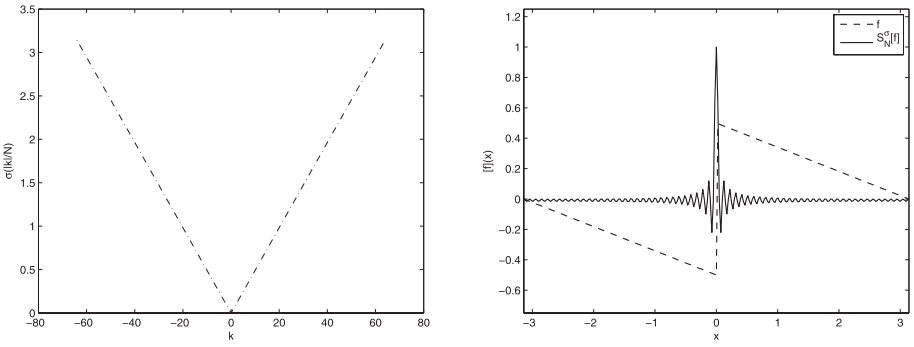

(a) Concentration Factor (b) Jump Response

Fig. 5 Problem Formulation 1, $N = 64$

problem formulation takes the form

$$\begin{aligned} \min_{\sigma} \quad & \phi_0(\sigma) \\ \text{subject to} \quad & \phi_m(\sigma) = c_m, \quad m = 1, \ldots, M \\ & \psi_n(\sigma) \le c_n, \quad n = 1, \ldots, N. \end{aligned} \tag{22}$$

The objective function ϕ_0 is typically a norm measure of $W_0^{\sigma,N}(x)$. c_m, c_n are constants or functions independent of σ while the constraints are typically functions of $W_i^{\sigma,N}(x)$ or σ. Sample problem formulations are discussed in Sect. 3.2. The computational complexity of the problem can be reduced by noting that σ is an even function. This follows from the admissibility condition requiring the concentration kernel (4) to be odd. Consequently, the design problem is an iterative program of size N rather than $2N + 1$.

All problem formulations which are discussed below are convex programs. Most are linear programs or quadratic programs with linear equalities and inequalities. In broad brush, they can all be formulated as second order cone programs (SOCPs), which can be solved using a variety of methods, [10]. In rare cases, problem formulations can lead to quasiconvex problems, which may necessitate other solution methods. In all simulations in this paper, we used CVX, a package for specifying and solving convex programs [11, 12]. Programs were implemented in Matlab (version 7.7) with CVX version 1.2 (build 711).

3.2 Sample Problem Formulations

The following problem formulations serve to illustrate the design framework.

1. Problem Formulation 1—*The (first-order) polynomial concentration factor*

   We start with a problem formulation minimizing the 2-norm of the jump waveform $W_0^{\sigma,N}(x)$, while ensuring its proper normalization.

$$\begin{aligned} \min_{\sigma} \quad & \| W_0^{\sigma,N} \|_2 \\ \text{subject to} \quad & W_0^{\sigma,N}\Big|_{x=0} = 1. \end{aligned} \tag{23}$$

   This results in a concentration factor and jump response as plotted in Fig. 5.

Journal ID: 10915, Article ID: 9524, Date: 2011-08-19, Proof No: 1, UNCORRECTED PROOF

« JOMP 10915 layout: Small Condensed v.1.2 file: jomp9524.tex (ELE) class: spr-small-v1.1 v.2011/08/17 Prn:2011/08/18; 11:21 p. 11/19»
« doctopic: OriginalPaper numbering style: ContentOnly reference style: mathphys»

By comparing Fig. 5 with Figs. 1 and 2, it is clear that this problem formulation results in the first-order polynomial concentration factor. This conjecture may be formalized in the following theorem:

Theorem 3.1 *Let $W_0^{\sigma,N}$ be the jump response. The concentration factor $\sigma(\eta) = \sigma\left(\frac{|k|}{N}\right)$ which solves the problem*

$$\begin{aligned} &\min_{\sigma} \quad \|W_0^{\sigma,N}\|_2 \\ &\textit{subject to} \quad W_0^{\sigma,N}\Big|_{x=0} = 1 \end{aligned} \tag{24}$$

is the first-order polynomial concentration factor, $\sigma_P^1(\eta) = \pi\eta$.

Proof By Parseval's relation, we have

$$\begin{aligned} \left\|W_0^{\sigma,N}\right\|_2 &= \left(\sum_{0<|k|\le N} \left|\frac{\sigma\left(\frac{|k|}{N}\right)\operatorname{sgn}(k)}{k}\right|^2\right)^{\frac{1}{2}} \\ &= \left(\sum_{0<|k|\le N} \left|\frac{\sigma\left(\frac{|k|}{N}\right)}{|k|}\right|^2\right)^{\frac{1}{2}}. \end{aligned} \tag{25}$$

By defining $\eta = \frac{|k|}{N}$, the above expression becomes

$$\left\|W_0^{\sigma,N}\right\|_2 = \frac{1}{N}\left(\sum_{0<\eta\le 1} \left|\frac{\sigma(\eta)}{\eta}\right|^2\right)^{\frac{1}{2}}. \tag{26}$$

The error is minimized when each term in the sum is minimized. Setting $\frac{d(\frac{\sigma(\eta)}{\eta})^2}{d\eta}$ to zero, we obtain

$$2\left(\frac{\sigma(\eta)}{\eta}\right)\cdot\left(\frac{\eta\sigma'(\eta) - \sigma(\eta)}{\eta^2}\right) = 0.$$

Since $\eta \neq 0$, we have

$$\eta\sigma'(\eta) = \sigma(\eta).$$

The solution of this equation takes the form

$$\sigma(\eta) = C\cdot\eta, \tag{27}$$

Journal ID: 10915, Article ID: 9524, Date: 2011-08-19, Proof No: 1, UNCORRECTED PROOF

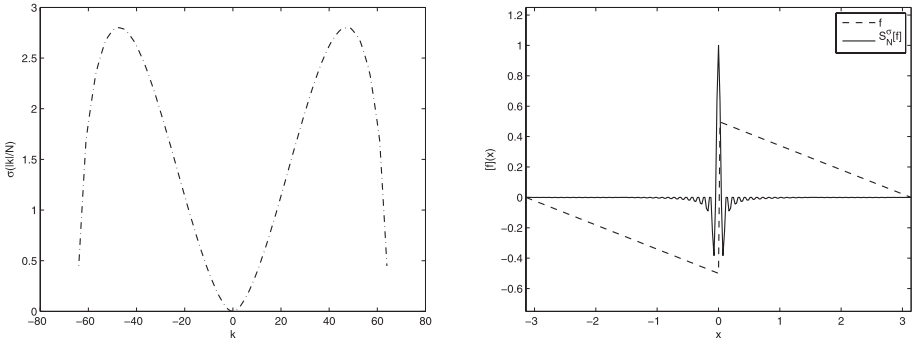

(a) Concentration Factor (b) Jump Response

Fig. 6 Problem Formulation 2, $N = 64$

where C is some constant. We determine C using the equality constraint, $W_0^{\sigma,N}|_{x=0} = 1$.

$$\begin{aligned} \frac{1}{2\pi} \sum_{0<|k|\le N} \frac{\sigma\left(\frac{|k|}{N}\right) \operatorname{sgn}(k)}{k} &= 1 \\ \frac{1}{\pi N} \sum_{\eta=1/N}^{1} \frac{\sigma(\eta)}{\eta} &= 1 \\ \frac{C}{\pi N} \cdot N &= 1 \\ C &= \pi. \end{aligned} \tag{28}$$

The result follows. □

2. Problem Formulation 2—*Sparse jump response*

The jump response of the polynomial concentration factor shows the presence of strong oscillatory behavior in the smooth regions away from the jumps. This can present a significant problem in identification of jumps by thresholding, leading to numerous false positives. We therefore consider a problem formulation where we minimize the 1-norm of the jump waveform $W_0^{\sigma,N}(x)$, subject to the usual normalization constraint.

$$\begin{aligned} \min_{\sigma} \quad & \|W_0^{\sigma,N}\|_1 \\ \text{subject to} \quad & W_0^{\sigma,N}\Big|_{x=0} = 1. \end{aligned} \tag{29}$$

This results in a concentration factor and jump response as plotted in Fig. 6.

As expected, the response in smooth regions is much smaller. The trade-off, however, is a decreased resolution of the actual jump and strong oscillatory sidelobes in the immediate vicinity of the jump. These features are illustrated in the plots of Fig. 7, which plots the absolute error between the true jump function and the concentration jump response on a logarithmic scale. The error plots for different values of N are provided to infer convergence

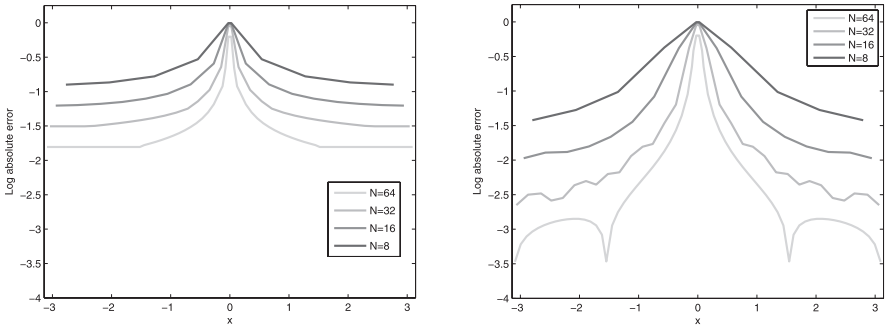

(a) Log Error for Problem Formulation 1 (b) Log Error for Problem Formulation 2

Fig. 7 Log absolute error between the true jump function and the concentration jump approximation, $N = 64$

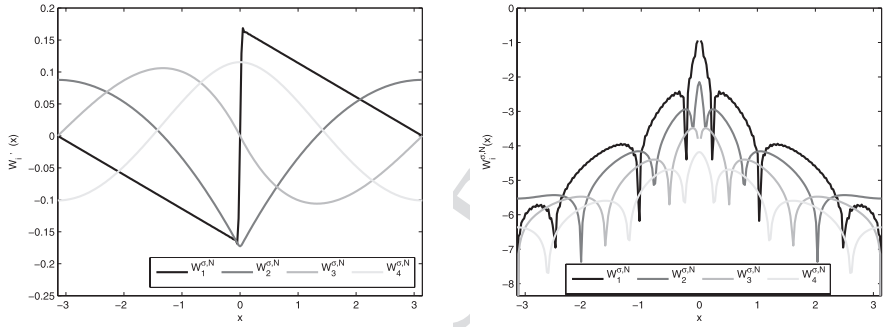

(a) Higher-order Kernels – Trigonometric Factor (b) Higher-order Kernels – Exponential Factor

Fig. 8 Plot of the higher-order kernels, $W_i^{\sigma,N}$, $i = 1, \ldots, 4$, $(N = 64)$

behavior. The almost flat error profile away from the jump in Fig. 7(a) (Problem Formulation 1) is a result of the slowly decaying oscillations. This is to be contrasted with the vanishing response in the same region in Fig. 7(b) (Problem Formulation 2).

3. Problem Formulation 3—*Higher order concentration factors*

   The previous problem formulations impose no constraints on the magnitude of the higher order kernels. From (20), we observe that this can present a problem when computing jump approximations for functions with significant variation and/or with jumps in higher-order derivatives. This was illustrated in Fig. 3(b), where the jump function approximations of $f_2(x)$ using the (low-order) trigonometric and (high-order) exponential concentration factors were plotted. For reference, we plot in Fig. 8 the first four higher-order kernels, $W_i^{\sigma,N}$, $i = 1, \ldots, 4$, for the trigonometric and exponential concentration factors respectively. Note the logarithmic scale and the significantly reduced values of the kernels for the exponential concentration factor.

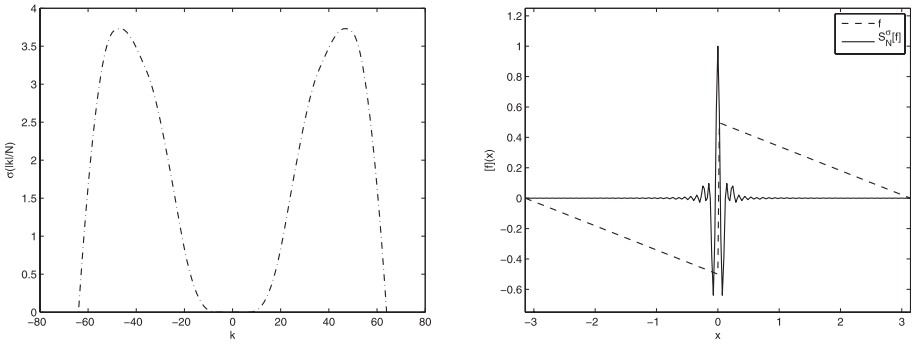

(a) Concentration Factor (b) Jump Response

Fig. 9 Problem Formulation 3, $N = 64$

With this in mind, we consider a problem formulation where we impose constraints on the higher-order kernels.[6]

$$\begin{aligned} \min_{\sigma} \quad & \|W_0^{\sigma,N}\|_1 \\ \text{subject to} \quad & W_0^{\sigma,N}\Big|_{x=0} = 1 \\ & \left\|W_1^{\sigma,N}\right\|_\infty \le 10^{-1} \\ & \left\|W_2^{\sigma,N}\right\|_\infty \le 10^{-3} \\ & \sigma \ge 0, \sigma(1) = 0. \end{aligned} \tag{30}$$

This results in a concentration factor and jump response as plotted in Fig. 9.

Its effectiveness in canceling out gradients and oscillations is illustrated in Fig. 10, which plots the response of the factors from problem formulations 2 and 3 respectively to the test function $f_2(x)$, (10). Problem Formulation 2 had no constraints on the higher order kernels; consequently, the jump response in Fig. 10(a) shows a significant non-zero value in the sinusoidal region. In contrast, this part of the jump response in Fig. 10(b) is near zero.[7] Such a concentration factor may be necessary in applications where functions with large variation are encountered, such as the solution of PDEs by spectral methods involving highly oscillatory solutions. Plots of the first four higher-order kernels corresponding to the two concentration factors are given in Fig. 11. Note the significantly smaller values for Problem Formulation 3. It is also illustrative to compare the performance of the factor from Problem Formulation 3 to the exponential concentration factor. The jump function approximations using the two factors are plotted in Fig. 3(b) and Fig. 10(b) respectively, while the plots of the higher-order kernels are provided in Fig. 8(b) and Fig. 11(b) respectively. We see that the concentration factor from the iterative formulation is more effective in canceling

[6] Ideally, the higher-order kernels should be vanishingly small. Programming constraints, however, make it difficult to do so.

[7] As before, the small oscillatory response in the vicinity of $x = -\frac{5\pi}{6}$ is due to the discontinuities in the derivative and higher-order derivatives of $f_2(x)$.

Journal ID: 10915, Article ID: 9524, Date: 2011-08-19, Proof No: 1, UNCORRECTED PROOF

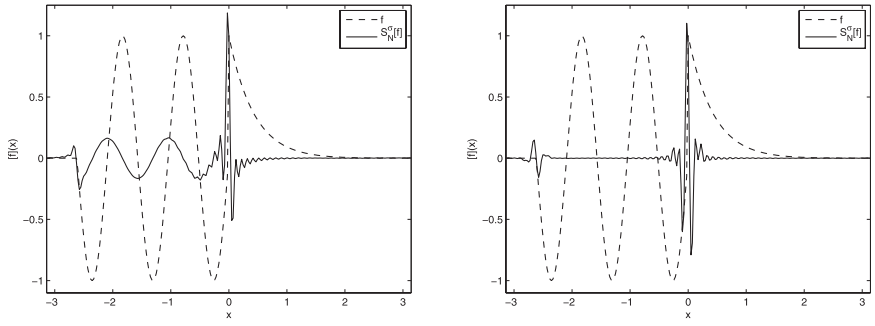

(a) Jump Approximation – Problem formulation 2 (Low order factor) (b) Jump Approximation – Problem formulation 3 (High order factor)

Fig. 10 Comparison of low and high-order concentration jump approximations, $N = 64$

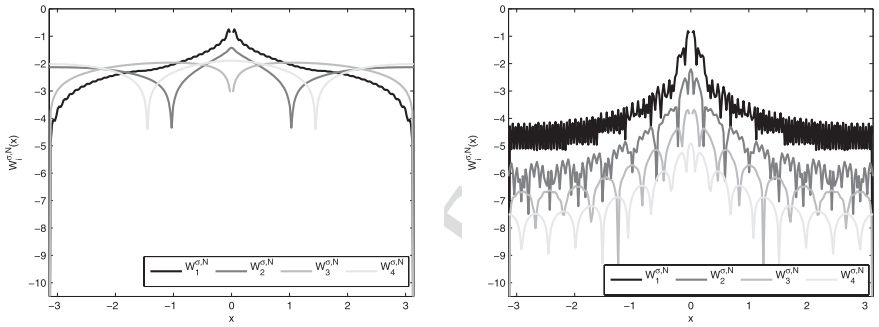

(a) Higher-order Kernels – Problem Formulation 2 (b) Higher-order Kernels – Problem Formulation 3

Fig. 11 Logarithmic plot of the higher-order kernels, $W_i^{\sigma,N}$, $i = 1, \ldots, 4$, $(N = 64)$

out the oscillatory response in the sinusoidal region. The underlying principle in the design of the two factors, is however, similar. The exponential factor was designed to cancel out as many moments as the order of the factor, [2]. Problem Formulation 3 serves the same purpose by canceling out several higher-order kernels. It is conceivable that a judicious choice of constraints in the iterative program will yield a solution numerically equivalent to the exponential concentration factor.

4. Problem Formulation 4

The method is also amenable to the imposition of other constraints. As an example, consider the following problem formulation, where we constrain the jump response to be small ($\mathcal{O}(10^{-4})$) beyond the immediate vicinity of the jump.

$$\begin{aligned} \min_{\sigma} \quad & \|W_0^{\sigma,N}\|_2 \\ \text{subject to} \quad & W_0^{\sigma,N}\Big|_{x=0} = 1 \\ & \left|W_0^{\sigma,N}\right|_{|x|\geq 0.2} \leq 10^{-4}. \end{aligned} \tag{31}$$

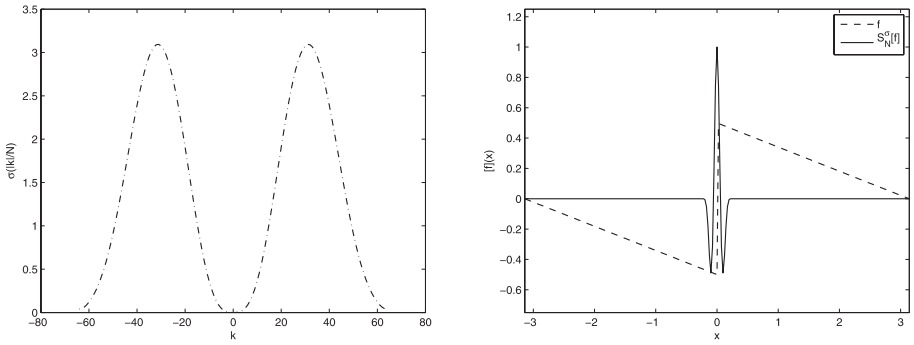

(a) Concentration Factor (b) Jump Response

Fig. 12 Problem Formulation 4, $N = 64$

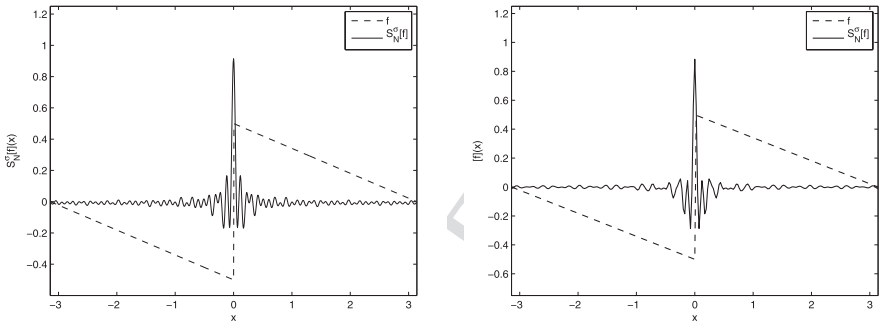

(a) Jump Response – Polynomial Factor (b) Jump Response – Problem Formulation 2

Fig. 13 Use of standard concentration factors with missing data, $N = 64$

This results in a concentration factor and jump response as plotted in Fig. 12. Note the clean jump response, with just one dominant sidelobe in the immediate vicinity of the jump.

4 Concentration Factor Design for Missing or Banded Spectral Data

This framework may also be utilized for the design of concentration factors with data missing certain coefficients. In particular, we will look into the problem of data missing measurements in spectral bands. This may be the case due to incidental or intentional narrowband interference, instrumentation errors or unreliable measurements in these bands. The use of standard concentration factors in these cases results in additional spurious oscillations throughout the reconstruction interval, as illustrated in Fig. 13. This figure plots the jump response to a unit ramp using the polynomial factor and the concentration factor designed in Problem Formulation 2. Fourier modes $\mathbb{K} = \{k | 30 \leq |k| \leq 40\}$ are assumed missing.

These additional spurious responses can lead to false jump detects, especially in the presence of noise. Hence, we use the design framework to explicitly specify the missing data as

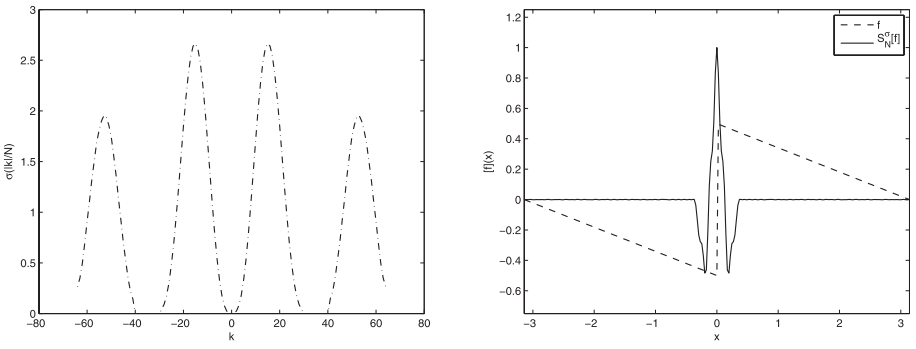

(a) Concentration Factor (b) Jump Response

Fig. 14 Concentration factor design for missing data, $N = 64$, modes 30–40 missing

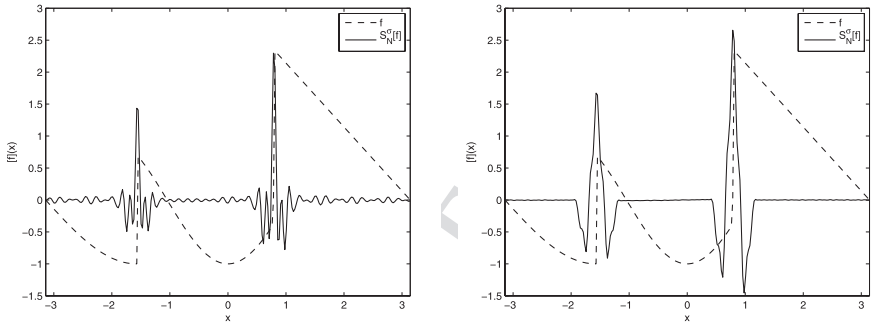

(a) Jump Approximation – Problem Formulation 2 (b) Jump Approximation – Concentration factor from solving (32)

Fig. 15 Jump approximation of $f_3(x)$ from its Fourier modes, $N = 64$, modes 30–40 missing

a constraint in the problem formulation, as in the following iterative program:

$$\begin{aligned} \min_{\sigma} \quad & \|W_0^{\sigma,N}\|_1 \\ \text{subject to} \quad & W_0^{\sigma,N}\Big|_{x=0} = 1 \\ & \sigma(\mathbb{K}) = 0 \\ & \left|W_0^{\sigma,N}\right|_{|x|\geq 0.35} \leq 10^{-3}. \end{aligned} \tag{32}$$

This results in a concentration factor and jump response as plotted in Fig. 14. Note the significantly reduced spurious oscillations away from the jump. The one consequence of the missing data, however, is the slightly reduced resolution of the jump itself. Also note that the iterative program implicitly imposes a degree of smoothness in the concentration factor in Fourier space.

Figure 15 plots the performance of the factor on the following test function.

$$f_3(x) = \begin{cases} \sin(x) & -\pi \le x < -\frac{\pi}{2} \\ -\cos\left(\frac{3x}{2}\right) & -\frac{\pi}{2} < x < \frac{\pi}{4} \\ \pi - x & \frac{\pi}{4} < x \le \pi. \end{cases} \tag{33}$$

$$[f]_3(x) = \begin{cases} \frac{\sqrt{2}+1}{\sqrt{2}} \approx 1.707 & x = -\frac{\pi}{2} \\ \frac{3\pi}{4} + \frac{1}{2}\sqrt{2-\sqrt{2}} \approx 2.734 & x = \frac{\pi}{4} \\ 0 & \text{else.} \end{cases} \tag{34}$$

The associated jump function is provided for reference in (34). As before, we note that the jump approximation is much cleaner. Moreover, with the standard concentration factors, the jump heights are not identified correctly. Recall (Sect. 2, admissibility conditions) that the concentration factors are required to satisfy a normalization constraint. This constraint is violated in the case of missing data, i.e., for the standard concentration factors

$$\sum_{\substack{k=1 \\ k \notin \mathbb{K}}}^{N} \frac{\sigma(\frac{|k|}{N})}{k} < \sum_{k=1}^{N} \frac{\sigma(\frac{|k|}{N})}{k} = 1. \tag{35}$$

Consequently, the jump response has the property that $W_0^{\sigma,N}(0) < 1$. This results in the jump height being incorrectly identified. It is only when the missing modes are explicitly modeled in the design process, the resulting concentration factor is suitably normalized, with

$$\sum_{\substack{k=1 \\ k \notin \mathbb{K}}}^{N} \frac{\sigma_{\text{mis}}(\frac{|k|}{N})}{k} = 1. \tag{36}$$

5 Concluding Remarks

In this paper, we have introduced an iterative framework for the design of concentration factors for use in edge detection from Fourier data. Some of the traditional concentration factors have been shown to be obtained as specific formulations of the design framework. We have also demonstrated the use of this framework for the design of concentration factors from Fourier data missing a band of modes. Thus designed concentration factors have been shown to provide cleaner jump approximations, as well as more accurate jump values.

Some avenues for future investigation remain, including the incorporation of statistical characteristics of noise in the design process. The extension of this framework to the design of multidimensional concentration factors is also a problem of significant interest and importance.

References

1. Gelb, A., Tadmor, E.: Detection of edges in spectral data. Appl. Comput. Harmon. Anal. **7**, 101–135 (1999)
2. Gelb, A., Tadmor, E.: Detection of edges in spectral data II. Nonlinear enhancement. SIAM J. Numer. Anal. **38**(4), 1389–1408 (2000)
3. Gelb, A., Tadmor, E.: Adaptive edge detectors for piecewise smooth data based on the minmod limiter. J. Sci. Comput. **28**(2–3), 279–306 (2006)
4. Gelb, A., Cates, D.M.: Detection of edges in spectral data III—refinement of the concentration method. J. Sci. Comput. **36**(1), 1–43 (2008)

5. Engelberg, S., Tadmor, E.: Recovery of edges from spectral data with noise—a new perspective. SIAM J. Numer. Anal. **46**(5), 2620–2635 (2008)
6. Archibald, R., Gelb, A.: Reducing the effects of noise in image reconstruction. J. Sci. Comput. **17**(1), 167–180 (2002)
7. Tadmor, E., Zou, J.: Novel edge detection methods for incomplete and noisy spectral data. J. Fourier Anal. Appl. **14**(5), 744–763 (2008)
8. Candes, E., Romberg, J., Tao, T.: Robust uncertainty principles: exact signal reconstruction from highly incomplete frequency information. IEEE Trans. Inf. Theory **52**, 489–509 (2004)
9. Candes, E., Romberg, J., Tao, T.: Stable signal recovery from incomplete and inaccurate measurements. Commun. Pure Appl. Math. **59**, 1207–1223 (2005)
10. Boyd, S.P., Vandenberghe, L.: Convex Optimization. Cambridge Univ. Press, Cambridge (2004)
11. Grant, M., Boyd, S.: CVX: Matlab software for disciplined convex programming (web page and software) (2008). http://stanford.edu/~boyd/cvx
12. Grant, M., Boyd, S.: Graph implementations for nonsmooth convex programs. In: Blondel, V., Boyd, S., Kimura, H. (eds.) Recent Advances in Learning and Control (a tribute to M. Vidyasagar). Lecture Notes in Control and Information Sciences, pp. 95–110. Springer, Berlin (2008)
13. Eckhoff, K.S.: Accurate and efficient reconstruction of discontinuous functions from truncated series expansions. Math. Comput. **61**(204), 745–763 (1993)